Journal of Organometallic Chemistry 1020 (2024) 123308

Contents lists available at ScienceDirect

Journal of Organometallic Chemistry

journal homepage: www.elsevier.com/locate/jorganchem

Revisiting the early days of conjugated polyyne synthesis. Syntheses and structures of Bis(triethylsilyl) Polyynediyl Adducts $Et_3Si(C{\equiv}C)_nSiEt_3$ previously regarded as Unisolable (n = 6, 8, 12)‡

Sourajit Dey Baksi, Aayushi Arora, Nattamai Bhuvanesh, Joseph H. Reibenspies, John A. Gladysz *

Department of Chemistry, Texas A&M University, PO Box 30012, College Station, Texas 77842-3012, USA

ARTICLE INFO

Keywords:
Polyynes
Trialkylsilylalkynes
Oxidative coupling
Crystal structures
X-ray powder diffraction
Hay coupling reaction
Cadiot-Chodkiewicz reaction

ABSTRACT

An overview of bis(trialkylsilyl) polyynediyl adducts $R_3Si(C{\equiv}C)_nSiR_3$ with $n \geq 5$ is followed by syntheses of **TESC$_x$TES** where x = 8, 12, 16, and 24 (**TES** = $SiEt_3$; $x = 2n$). In a seminal 1972 study, the last three were presented as too unstable to isolate and thus only characterized by UV-visible spectroscopy. Although not a rational route, **TESC$_{24}$TES** is consistently obtained from the reaction of *trans*-$(C_6F_5)(p\text{-}tol_3P)_2Pt(C{\equiv}C)_5SiEt_3$ and crude **HC$_8$TES** under Hay oxidative cross coupling conditions. The latter contains some **HC$_8$H** and **TESC$_8$TES**. Hay oxidative homocouplings of **HC$_4$TES** and crude **HC$_8$TES** afford **TESC$_8$TES** (83%) and **TESC$_{16}$TES** (5%). A Cadiot-Chodkiewicz reaction of **BrC$_4$Br** and **HC$_4$TES** (2 equiv) yields **TESC$_{12}$TES** (11%). All of these compounds are crystalline, and the crystal structures of **TESC$_8$TES** and **TESC$_{16}$TES** are determined. The $^{13}C\{^1H\}$ NMR and UV-visible properties are also compared.

1. Introduction

The synthesis of extended conjugated polyynes, defined for the purposes of this paper as consisting of five or more triple bonds ($C_{\geq 10}$), has been of great interest in a variety of contexts [1]. Some of these involve modeling the polymeric sp carbon allotrope carbyne [2], in particular its electronic structure. Others relate to the many synthetic challenges associated with preparing monodisperse samples with very high sp chain lengths C_x (x = 40-52 and beyond) [3-5]. Polyynes also provide opportunities for syntheses of new carbon-based materials [6], a subject in its infancy from the standpoint of machine-generatable C_x precursors [7].

Much of the foundation of this field was laid some 52 years ago with the seminal work of Walton and his coworkers [8-9], although other earlier contributors merit note in passing [10]. Walton's exploratory studies were carried out in an era where ^{13}C NMR spectroscopy was not yet a routine tool, and his increasingly labile higher polyynes were characterized solely by UV-visible spectroscopy *in situ*. Walton sought a library of compounds with triethylsilyl endgroups, **TESC$_x$TES**, as represented in Scheme 1. One key building block was **HC$_4$TES**, which can be prepared on multigram scales and could be oxidatively homocoupled under Hay conditions [11] to give **TESC$_8$TES**, or cross coupled with **HC$_2$TES** to give **TESC$_6$TES**. These are the last polyynes in this series that can be considered "fully characterized" apart from NMR data (mp, IR and UV-visible spectroscopy, mass spectrometry, microanalysis) [8].

When Walton attempted monoprotodesilylations of **TESC$_x$TES** (x = 6, 8), mixtures of **HC$_x$H, HC$_x$TES**, and **TESC$_x$TES** formed. Nonetheless, after column chromatography, solutions enriched in **HC$_x$TES** could be obtained in unspecified yields. These were oxidatively homocoupled to **TESC$_{12}$TES** and **TESC$_{16}$TES**, which were reported to rapidly decompose at 20°C and –20°C, respectively, although the latter could be obtained as white crystals upon solvent removal at –30°C. Subsequent desilylations afforded solutions of **HC$_{12}$TES** and **HC$_{16}$TES**, with a 36% yield assigned to the latter based upon an estimated extinction coefficient of a UV-visible band. These were oxidatively homocoupled to solutions of **TESC$_{24}$TES** and **TESC$_{32}$TES**, with some **HC$_{16}$TES** persisting in the latter. Relevant to other topics below, a **TESC$_{20}$TES** solution was prepared by the oxidative cross coupling of **HC$_{16}$TES** and **HC$_4$TES**. Related cross couplings afforded **TESC$_{10}$TES, TESC$_{14}$TES**, and **TESC$_{18}$TES**, sometimes with trace impurities.

‡ This article is dedicated with great affection to Prof. Dr. Thomas Strassner on the occasion of his 60th birthday.

* Corresponding author. John A. Gladysz.
E-mail address: gladysz@mail.chem.tamu.edu (J.A. Gladysz).

https://doi.org/10.1016/j.jorganchem.2024.123308
Received 2 July 2024; Received in revised form 8 August 2024; Accepted 10 August 2024
Available online 22 August 2024

Since Walton's time, polyynes with trialkylsilyl endgroups have played a considerable role in the development of this field. Subsequently studied series are depicted in Scheme 1 [12-15]. The first and most extensive, with tri(isopropyl)silyl endgroups (**TIPSC$_x$TIPS**), has been chiefly elaborated by Tykwinski [12], with supporting contributions from Anderson [13] and other researchers and their teams [14,16]. In sharp contrast to Walton's polyyne portfolio, **TIPSC$_{20}$TIPS** was easily isolated and stable to 105°C. A DSC exotherm indicated decomposition near 123°C. The greatly enhanced stability versus **TESC$_{20}$TES** was attributed to the increased bulk of the TIPS endgroup. Aryl-substituted silicon endgroups (SiR_2Ar, $SiRAr_2$, $SiAr_3$) would also seem to have promise, but to our knowledge none have yet been installed on pentaynes or higher homologs [17].

In developing this chemistry, reactions other than those applied by Walton were often employed, such as the Fritsch-Buttenberg-Wiechell rearrangement used to access certain lower homologs of **TIPSC$_{20}$TIPS**. The route reported by Goroff and coworkers for the bis(trimethylsilyl) adduct **TMSC$_{10}$TMS**, a three-component coupling of **IC$_6$I** and **TMSC$_2$TMSn** (2×, **TMSn** = $SnMe_3$; cat. *trans*-$Pd(PPh_3)_2Cl_2$/CuI, 60%) [15a], is relevant to a synthesis given below. Under similar conditions, the reaction of the digold complex **Ph$_3$PAuC$_6$AuPPh$_3$** and **IC$_2$TMS** (2×) also gives **TMSC$_{10}$TMS** (38%) [15b].

We recently detailed a series of cross coupling reactions using Walton's eight carbon building block **HC$_8$TES**, as exemplified in Scheme 2 [4,8]. These studies were directed at diplatinum polyynediyl complexes with sp carbon chains as long as C_{52}. During certain procedures, minor polyyne byproducts consistently formed but were removed under workup conditions. These carried TES endgroups, were commonly crystalline, and challenged conventional dogma regarding Walton's compounds. In this paper, we present a modernized description and characterization of polyynes of the formula **TESC$_x$TES** (x = 24, 16, 12).

2. Results

2.1. Syntheses

For this section, a roughly chronological structure is employed. In the published conversion of **PtC$_{10}$TES** to **PtC$_{18}$TES** and **PtC$_{26}$TES** in Scheme 2 (**Pt** = *trans*-$(C_6F_5)(p\text{-}tol_3P)_2Pt$), a large excess of the cross coupling partner **HC$_8$TES** was used. The **PtC$_{26}$TES** is most economically viewed as arising from an *in situ* protodesilylation of **PtC$_{18}$TES** followed by a second coupling with **HC$_8$TES**, but there are other possibilities. This was a key stockpiling step en route to **PtC$_{52}$Pt** [4], and the yield ranges represent multiple runs.

As shown in Scheme 3, the **HC$_8$TES** is generated from **TESC$_8$TES** [4,8,18] by our version of Walton's protocol, which has been previously reported but is reproduced in the supporting information (SI) [4]. The samples contain **HC$_8$H** and **TESC$_8$TES**, and in exploratory work a subsequent (partial) chromatographic purification was carried out, parallel to Walton [19]. However it was later found that comparable yields of the platinum products in Scheme 2 could be obtained using the **HC$_8$H/HC$_8$TES/TESC$_8$TES** mixture (termed "crude **HC$_8$TES**") directly.

In one such run, a chromatographic workup at <10°C gave **PtC$_{18}$TES** (16%) and **PtC$_{26}$TES** (7%) as previously disclosed, and additionally **TESC$_{24}$TES**. The molar quantity obtained was close to that of the two platinum products summed, but the formal yield was lower as it must be based upon **HC$_8$TES** (4%, see experimental section). Although **TESC$_{24}$TES** was easily isolated as a bright orange microcrystalline solid, it slowly turned brown and then black over the course of an hour at room temperature. Thus, it was stored at –35°C and could be kept in CH_2Cl_2 solutions at this temperature for at least 2 weeks.

The reproducible generation of **TESC$_{24}$TES** in Scheme 2 presents an interesting mechanistic puzzle. Given the five triple bonds in the platinum educt **PtC$_{10}$TES**, and twelve in **TESC$_{24}$TES**, it is highly unlikely that the former is involved. Perhaps **HC$_8$H** can cross couple with two equivalents of **HC$_8$TES**. But the homocoupling of **HC$_8$TES** to give **TESC$_{16}$TES** would seem nearly equally likely. Possibly the fluoride ion unique to this sequence plays a role.

Although Walton reported that **TESC$_{16}$TES** decomposed at –20°C, we were emboldened by the stability of **TESC$_{24}$TES** and attempted a Hay oxidative homocoupling [11] of "crude **HC$_8$TES**". As shown in Scheme 3 (bottom), workup at room temperature gave **TESC$_{16}$TES** as air stable orange needles in 5% yield, as calculated in the experimental section. Interestingly, no **TESC$_{24}$TES** was detected, including mass spectrometric assays. The sample was low melting (36°C), but displayed no special thermal instability. If it had been produced in Scheme 2, it would have eluted close to **PtC$_{26}$TES**.

In connection with another research project [20], an authentic sample and $^{13}C\{^1H\}$ NMR spectrum of **TESC$_{12}$TES** was required. Consideration was given to repeating Walton's route, with the idea that a stable product could be obtained from his solutions. However, the yield of the precursor **TESC$_6$TES** was not specified, and the subsequent monodesilylation to **HC$_6$TES** was noted as poorly selective above. Alternative preparative routes to **HC$_6$TES** could not be found in the literature [21]. Thus, the assembly of **TESC$_{12}$TES** from four readily available C_4 precursors was attempted. As shown in Scheme 4, the

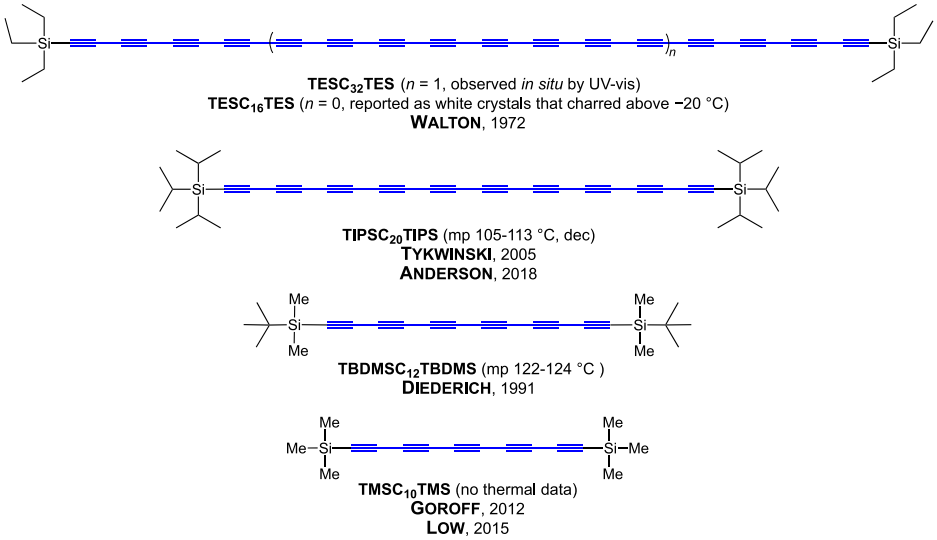

Scheme 1. Classes of conjugated polyynes (C_{10} and higher) with trialkylsilyl endgroups.

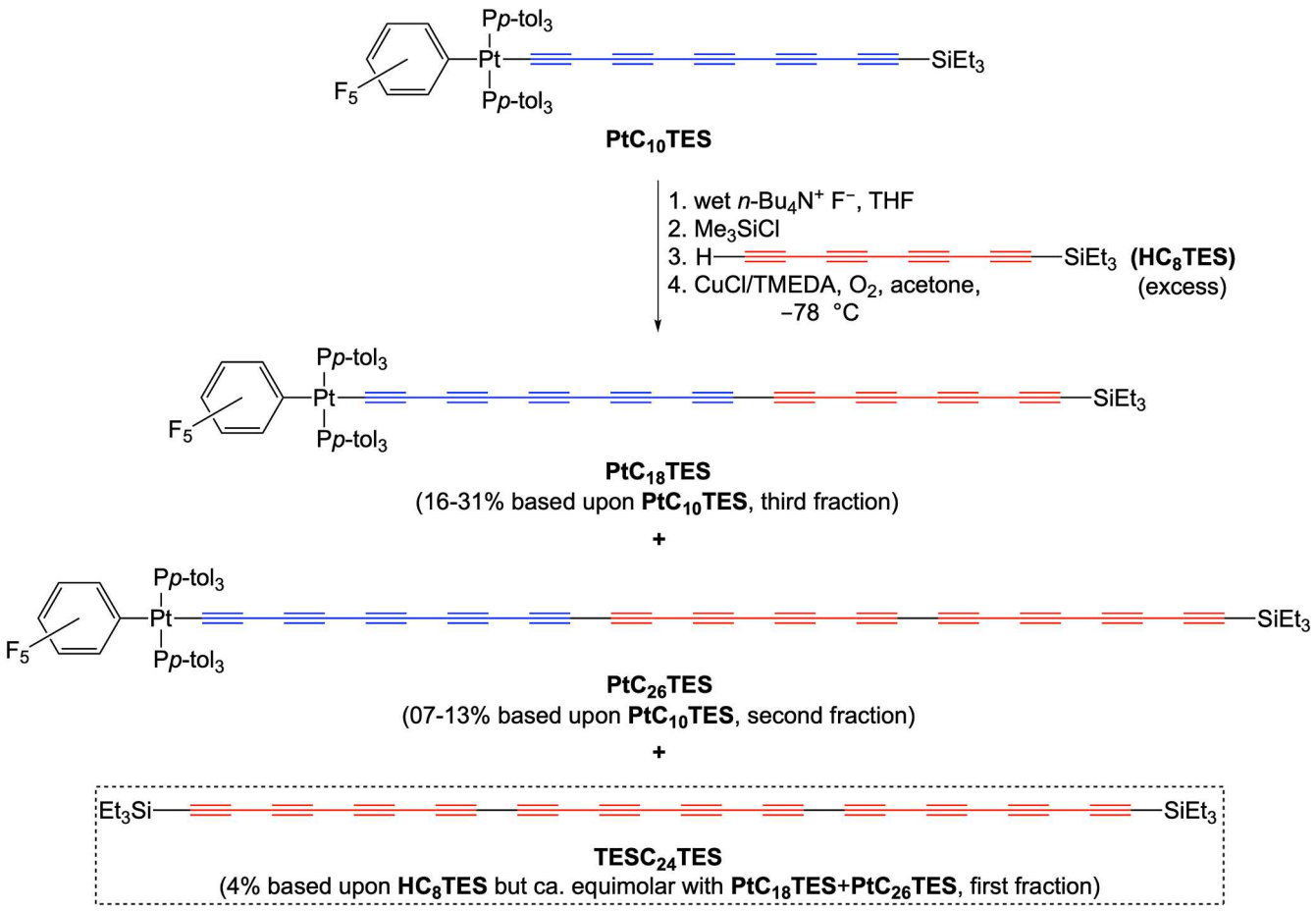

Scheme 2. Cross coupling reactions that yield **TESC$_{24}$TES** as byproduct.

brominated diyne **BrC$_4$Br** [22] was condensed with 2.2 equiv of **HC$_4$TES** under Cadiot-Chodkiewicz conditions [23]. This can be viewed as a palladium and copper catalyzed HBr elimination, aided by stoichiometric quantities of an amine base. Although the yield of **TESC$_{12}$TES** was modest (11%), in part due to the competing formation of **TESC$_8$TES** (2% based upon **HC$_4$TES**), the quantities sufficed for our purposes.

2.2. Physical characterization

The three newly isolated compounds, **TESC$_{12}$TES, TESC$_{16}$TES**, and **TESC$_{24}$TES**, were characterized by NMR (^{1}H, ^{13}C{^{1}H}) and UV-visible spectroscopy and mass spectrometry. NMR spectra that indicate high purities are provided in the SI. Key ^{13}C{^{1}H} NMR data are summarized in Table 1, together with literature data for lower homologs [24] to better illustrate monotonic chemical shift trends. These are in quite close agreement with those seen by Tykwinski with **TIPSC$_x$TIPS**. The Si*C*≡*C* signals of the platinum complexes **PtC$_x$TES** are also included in Table 1, and show the weakening influence of platinum as the sp chain elongates.

UV-visible spectra recorded in CH_2Cl_2 or hexane are summarized in Table 2. The λ_{max} and ε values for **TESC$_8$TES, TESC$_{12}$TES, TESC$_{16}$TES** are in very good agreement with Tykwinski's analogs **TIPSC$_8$TIPS, TIPSC$_{12}$TIPS**, and **TIPSC$_{16}$TIPS** [12]. Walton observed similar λ_{max} values, as documented in the footnotes in Table 2, and molar extinction coefficients generally followed parallel trends. The most pronounced differences were with low intensity bands associated with **TESC$_8$TES**. These have a special origin [1b,25,26] and were less evident in our initial spectra. However, when concentrations were increased ca. 100-fold (Table 2), they became clearly visible. As a check, a comparable spectrum of **TIPSC$_8$TIPS** was recorded, and a similar series of bands observed.

All of our compounds showed signs of crystallinity. Crystals of **TESC$_{16}$TES** and **TESC$_8$TES** suitable for X-ray diffraction could be grown. Despite much effort over many months, **TESC$_{24}$TES** proved to be a "near miss", but powder X-ray diffraction verified the crystalline nature of the samples (Fig. s1). The structures of **TESC$_8$TES** and **TESC$_{16}$TES** could be solved as summarized in Table 3 and the experimental section. The latter exhibited two independent molecules in the unit cell. Thermal ellipsoid plots are provided in Fig. 1, and key metrical parameters are summarized in Table 4.

3. Discussion

The above data provide a reset on the way Walton's extensive studies of **TESC$_x$TES** are viewed. With the likely exception of **TESC$_{32}$TES**, all of his polyynes described in the introduction should now be regarded as isolable. There are many cases where over the course of time, advances in techniques, instrumentation, and experimental sophistication have led to breakthroughs in isolating compounds previously regarded as unstable or labile. Walton's syntheses have an advantage in their systematic nature. In contrast, our routes to **TESC$_x$TES** (Schemes 2-4) approach such molecules from three different directions, and the preparatively impractical yields leave much to be desired.

There are now a fair number of crystal structures of extended polyynes in the literature, with the longest being **PtC$_{24}$Pt** for symmetrical substitution and **PtC$_{26}$TES** for unsymmetrical [4,27]. The structures in Fig. 1 do not exhibit any new phenomena, but the raw data are of value, as they enable statistically sounder experimental conclusions regarding bond length alternation (BLA), a key question as the sp chains are extended. The most commonly used BLA parameters are included in Table 4. Tykwinski was able to obtain a number of crystal structures in

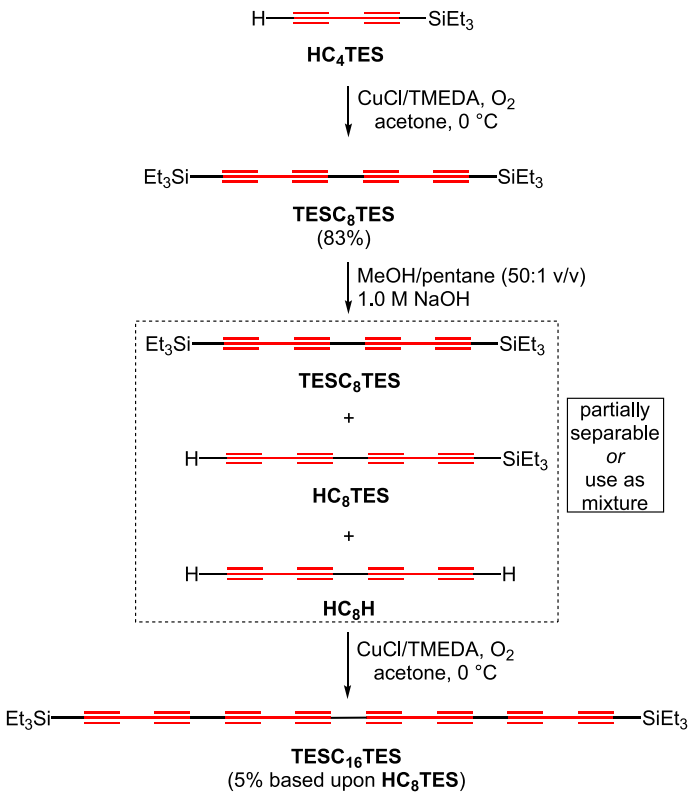

Scheme 3. Syntheses of **TESC$_8$TES**, **HC$_8$TES**, and **TESC$_{16}$TES**.

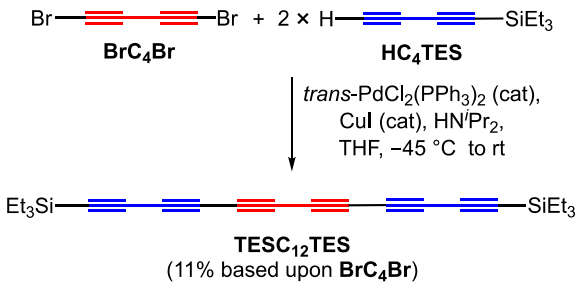

Scheme 4. Synthesis of **TESC$_{12}$TES**.

Table 1
$^{13}C\{^1H\}$ NMR data (*sp* signals only, δ/ppm, 126 MHz/$CDCl_3$) for **TESC$_x$TES** and analogous monoplatinum compounds **PtC$_x$TES**.

compound	Si<u>C</u>≡C	Si<u>C</u>≡<u>C</u>	others
TESC$_2$TES[a]	113.1	–	–
TESC$_4$TES[b]	83.3	89.4	–
TESC$_8$TES[c]	86.5	89.0	62.3, 61.8
TESC$_{12}$TES[c]	87.8	88.9	62.8, 62.7, 62.6, 61.7
TESC$_{16}$TES	88.3	88.7	63.3, 63.1, 63.0, 62.7, 62.5, 61.6
TESC$_{24}$TES	88.7	88.7	63.9, 63.8, 63.6, 63.5, 63.4, 63.1, 62.9, 62.5, 62.4, 61.5
PtC$_8$TES[d]	82.9	90.2	see reference [4]
PtC$_{12}$TES[d]	86.2	89.4	see reference [4]
PtC$_{16}$TES[d]	87.6	89.0	see reference [4]
PtC$_{24}$TES[d]	88.5	88.8	see reference [4]

[a] Data in C_6D_6 from reference [24a].
[b] Data from reference [24b] and independently confirmed in this study.
[c] Data in CD_2Cl_2 (δ/ppm, *sp* signals only): **TESC$_8$TES** 87.3, 88.9, 62.4, and 61.6; **TESC$_{12}$TES** 88.6, 88.7, 63.0, 62.9, 62.6, and 61.5.
[d] Data from reference [4].

the **TIPSC$_x$TIPS** series [12], the most relevant being the octayne **TIPSC$_{16}$TIPS** and tetrayne **TIPSC$_8$TIPS**, the counterparts of the two structures in Fig. 1. These exhibited packing motifs different from those of the TES analogs, as reflected by different space groups or values of *Z*. Tykwinski's work also included a careful analysis of $^{13}C\{^1H\}$ NMR spectra, and the chemical shift trends in Table 1 are virtually superimposable upon his.

Bulky endgroups are widely viewed as contributing to the stability of extended polyynes [1,3-5,12,22]. The sp chains are generally regarded as the loci of decomposition, and gigantic substituents sterically enforce greater chain/chain separations. Tykwinski carefully assayed the stabilities of **TIPSC$_x$TIPS** (x = 6, 8, 10, 12, 16, 20) by DSC and capillary thermolyses. The octayne **TIPSC$_{16}$TIPS** melted at 93-95°C and decomposed near 132°C (DSC), whereas **TESC$_{16}$TES** melts at 36°C and decomposes at 106°C (closed capillary). In any case, despite the upward revision of the stabilities of **TESC$_x$TES**, we still believe in the operation of a steric effect that renders the TIPS adducts somewhat more stable.

To sum, there is now a much clearer picture of the isolabilities and stabilities of bis(triethylsilyl) adducts of polyynes. However, there remains much room for improvement in synthetic methodologies. Towards this end, we have recently developed new (C≡C)$_n$SiR$_3$ coupling reactions that proceed in high yields at room temperature and hold promise for the generation of still longer **TESC$_x$TES** assemblies [20].

4. Experimental section

4.1. General data

Reactions were conducted under dry inert atmospheres using conventional Schlenk techniques, but workups were carried out in air. Chemicals were treated as follows: THF, hexanes, diethyl ether, and CH_2Cl_2, passed through a Glass Contour solvent purification system; acetone, treated with CaH_2; pentane, MeOH, EtOH (3 × ACS grade), CuCl (99%/Alfa Aesar or 98%/Acros), CuI (99%/Acros), TMEDA (Alfa Aesar), *trans*-$Pd(PPh_3)_2Cl_2$ (98%/Sigma-Aldrich), HN^iPr_2 (99+%/Alfa

Table 2
UV-visible data for **TESC$_x$TES** and **TIPSC$_x$TIPS**.

compound	solvent	conc. (mol/L)	wavelength (nm) [ε ($M^{-1}cm^{-1}$)]
TESC$_8$TES[a,b]	CH_2Cl_2	1.02 × 10^{-5}	258 [266000], 236 [166000], 224 [77600]
TESC$_8$TES[b,c]	CH_2Cl_2	4.6 × 10^{-3}	390 [45], 377 [70], 366 [109], 351 [130], 336 [490], 317 [600], 298 [790], 284 [750], 281 [840], 270 [745], 261 [843][c]
TESC$_{12}$TES[a,d]	CH_2Cl_2	1.12 × 10^{-5}	303 [314000], 287 [281000], 269 [156000], 256 [60000], 244 [29100]
TESC$_{16}$TES[a,e]	CH_2Cl_2	2.15 × 10^{-5}	341 [513000], 322 [403000], 302 [187000], 282 [78000], 267 [26500]
TESC$_{24}$TES[f,g]	CH_2Cl_2	1.08 × 10^{-6}	406 [521000], 373 [411000], 342 [211000], 323 [77000], 306 [23400]
TIPSC$_8$TIPS[h]	hexanes	–	260 [157000], 248 [130000], 239 [84000]
TIPSC$_8$TIPS[c,h]	hexanes	1.82 × 10^{-3}	378 [187], 371 [163], 351 [278], 345 [254], 327 [286], 320 [286], 303 [852], 285 [824], 275 [1965][c]
TIPSC$_{12}$TIPS[h]	hexanes	–	304 [359000], 286 [262000], 271 [112000], 258 [43100], 245 [24200]
TIPSC$_{16}$TIPS[h]	hexanes	–	339 [603000], 319 [505000], 301 [237000], 285 [89200], 271 [31700]

[a] The log[ε] values reported by Walton in Table 2 of reference [8] for **TESC$_x$TES** (x = 8, 12, 16) have been converted to ε for comparison purposes.
[b] Data of Walton from reference [8] (λ_{max}, [ε], hexane): 376 (109), 370 (89), 361 (30), 349 (190), 345 (151), 336 (40), 326 (151), 322 (141), 314 (40), 257 (270000), 244 (186000) 232 (66000) 222 (21000).
[c] Data for the more intense bands at longer wavelengths could not be accurately determined at this elevated concentration; please refer to the more dilute (preceding) sample.
[d] Data of Walton from reference [8] (λ_{max}, [ε], hexane): 299 (407000), 283 (324000), 268 (129000), 254 (42700), 242 (41700).
[e] Data of Walton from reference [8] (λ_{max}, [ε], hexane): 336 (447000), 316 (398000), 299 (182000), 283 (56200), 270 (19900).
[f] Data of Walton from reference [8] (λ_{max}, hexane): 390, 365, 343, 325, 309.
[g] Due to the quantity of sample available, the concentration and ε value is considered accurate to only two significant digits.
[h] Data from reference [12].

Table 3
Summary of crystallographic data.

	TESC$_8$TES	**TESC$_{16}$TES**
empirical formula	$C_{20}H_{30}Si_2$	$C_{28}H_{30}Si_2$
formula weight	326.62	422.70
temperature [K]	110.0	110.0
diffractometer	Bruker Venture	Bruker Venture
wavelength [Å]	1.54178	1.54178
crystal system	orthorhombic	triclinic
space group	$Pca2_1$	P-1
unit cell dimensions		
a [Å]	19.3910(9)	7.2835(3)
b [Å]	8.0666(4)	14.4399(7)
c [Å]	13.6638(7)	25.7214(11)
α [°]	90	89.423(2)
β [°]	90	88.525(2)
γ [°]	90	75.824(2)
volume [Å^3]	2137.28(18)	2621.9(2)
Z/Z'	4/1	4/2
ρ_{calc} [Mg/m^3]	1.015	1.071
μ [nm^{-1}]	1.452	1.293
F(000)	2064	904
crystal size [mm]	0.28 × 0.15 × 0.05	0.14 × 0.03 × 0.03
Θ range [°]	4.560 to 70.108	1.718 to 70.625
index ranges	$-23 \le h \le 23$ $-9 \le k \le 9$ $-16 \le l \le 16$	$-8 \le h \le 8$ $-17 \le k \le 17$ $-31 \le l \le 31$
reflections collected	23344	48209
independent reflections	4044 [R(int) = 0.0440]	9977 [R(int) = 0.0446]
data/restraints/parameters	3880/1/205	8778/0/553
goodness-of-fit on F^2	1.144	1.076
final R indices [I>2σ(I)]	$R1$ = 0.0340, wR^2 = 0.0843	$R1$ = 0.0561, wR^2 = 0.1382
R indices (all data)	$R1$ = 0.0366, wR^2 = 0.0868	$R1$ = 0.0636, wR^2 = 0.1441
largest diff. peak/hole [eÅ^{-3}]	0.239 and −0.171	0.845 and −0.506

Aesar), Me_3SiCl (Sigma-Aldrich), NaOH (98%/Sigma-Aldrich), HCl (97%/ Sigma-Aldrich), n-$Bu_4N^+F^-$ (1.0 M in THF, 5 wt% water/Acros), $CDCl_3$ (Cambridge Isotope Laboratories), $MgSO_4$ (Fisher Chemical), and silica gel (Acros, Fluoroflash or 60M Macherey-Nagel), used as received.

NMR spectra were obtained on standard 500 MHz spectrometers and referenced as follows (δ/ppm): ^{1}H, residual $CHCl_3$ (7.24); $^{13}C\{^1H\}$, internal $CDCl_3$ (77.0). Mass spectra were recorded using a Thermo Scientific Q Exactive Focus (APCI) instrument. Thin-layer chromatography (TLC) was carried out on EMD Silica Gel 60 F_{254} aluminum plates and visualized using 254 or 365 nm lamps.

5. Caution

Polyynes normally possess highly positive heats of formation and may be regarded as energy-rich materials that are intrinsically thermodynamically unstable. Many explosions or rapid exothermic decompositions of polyynes have been reported [28]. These most frequently involve species with $(C{\equiv}C)_nX$ linkages (X = H, halide, $n > 2$). Regardless, all polyynes should be treated as potentially explosive and appropriate safety precautions taken.

5.1. *TESC$_{12}$TES*

A Schlenk flask was charged with **BrC$_4$Br** (0.212 g, 1.03 mmol) [22], **HC$_4$TES** (0.373 g, 2.27 mmol) [27], *trans*-$Pd(PPh_3)_2Cl_2$ (0.0029 g, 0.0041 mmol), CuI (0.0016 g, 0.0082 mmol), and THF (30 mL) with stirring, and cooled to −45°C (dry ice/acetonitrile). After 0.5 h, $HNiPr_2$ (0.4 mL) was added. After 2 h (TLC showed no remaining educt), the mixture was warmed to rt and diethyl ether (15 mL) and saturated aqueous NH_4Cl (15 mL) were added. The organic layer was separated, washed with H_2O (2 × 15 mL) and brine (1 × 15 mL), and dried ($MgSO_4$). The solvents were removed by rotary evaporation (0°C) to give a brownish oil. The residue was dry-loaded on a silica gel column (2 × 20 cm, packed in hexanes, ice-jacketed) and eluted with hexanes to give (following rotary evaporation at <10°C) first **TESC$_{12}$TES** as an orange-yellow oil (0.0269 g, 0.072 mmol, 7% based upon **BrC$_4$Br**) and then **TESC$_8$TES** as a yellow oil (0.035 g, 0.027 mmol, 2% based upon **HC$_4$TES**). Additional **TESC$_{12}$TES** was recovered from intermediate fractions by preparative TLC (silica gel, hexanes; 0.0154 g, 0.0412 mmol, 4% following rotary evaporation at <10°C). MeOH was added to the combined oily residues at 4°C, which gave **TESC$_{12}$TES** as a dark yellow powder, which was collected by vacuum filtration (11% total yield), mp 45°C (open capillary).

NMR (δ/ppm, $CDCl_3$): ^{1}H (500 MHz) 0.99 (t, $^3J_{HH}$ = 7.8 Hz, 18H, CH_3), 0.65 (q, $^3J_{HH}$ = 7.9 Hz, 12H, $SiCH_2$); $^{13}C\{^1H\}$ (126 MHz, cryoprobe) 88.9 (s, $C{\equiv}CSi$) [29], 87.8 (s, $C{\equiv}CSi$) [29], 62.8, 62.7, 62.6, 61.7 (4 s, $SiC{\equiv}C(C{\equiv}C)_3$), 7.4 (s, $SiCH_2CH_3$), 4.2 (s, $^1J_{CSi}$ = 56.6 Hz [30], $SiCH_2$); NMR (δ/ppm, CD_2Cl_2): ^{1}H (500 MHz) 1.00 (t, $^3J_{HH}$ = 7.8 Hz, 18H, CH_3), 0.66 (q, $^3J_{HH}$ = 7.9 Hz, 12H, $SiCH_2$); $^{13}C\{^1H\}$ (126 MHz, cryoprobe) 88.7 (s, $C{\equiv}CSi$) [29], 88.6 (s, $C{\equiv}CSi$) [29], 63.0, 62.9, 62.6, 61.5 (4 s, $SiC{\equiv}C(C{\equiv}CCCC)_2$), 7.5 (s, $SiCH_2CH_3$), 4.4 (s, $^1J_{CSi}$ = 56.7 Hz [30], $SiCH_2$).

IR (powder film, cm^{-1}) 2147/2033 (m/m, $\nu_{C{\equiv}C}$). MS ($APCI^-$) [31]: 374 ([**TESC$_{12}$TES**]$^-$, 100%).

5.2. *TESC$_{16}$TES*

A three-neck round-bottom flask was fitted with a gas dispersion tube, charged with "crude **HC$_8$TES**" (see SI; from 8.97 mmol of **TESC$_8$TES** and in ca. 30 mL of pentane; ca. 3 mmol of **HC$_8$TES**) and acetone (150 mL) and cooled to 0°C. A Schlenk flask was charged with

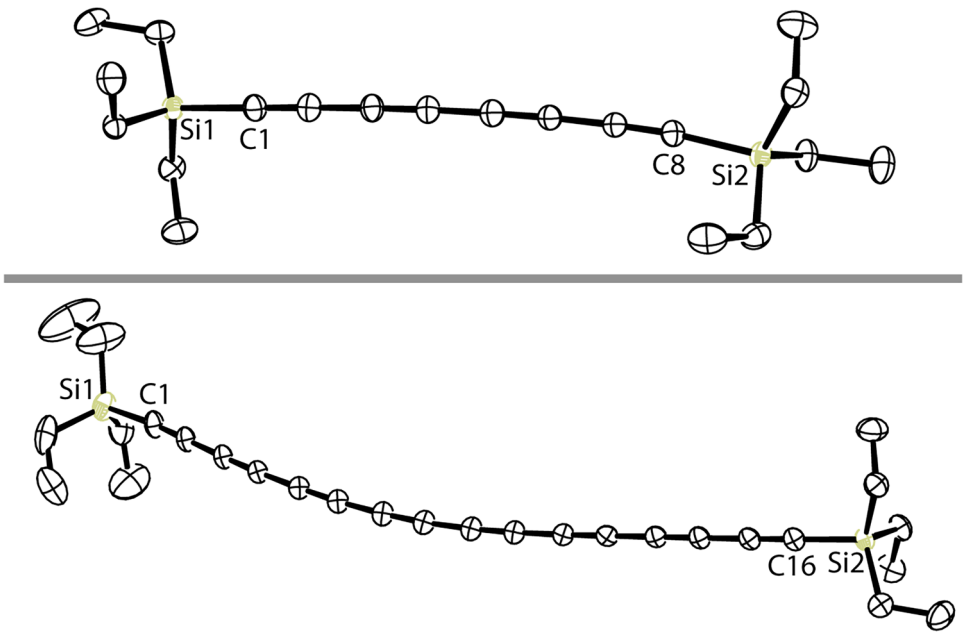

Fig. 1. Thermal ellipsoid plots (50% probability level) for **TESC$_8$TES** and **TESC$_{16}$TES** with hydrogen atoms omitted. For **TESC$_{16}$TES**, only one of the two independent molecules in the unit cell is shown.

CuCl (0.750 g, 7.58 mmol), acetone (20 ml), and TMEDA (0.375 mL, 0.291 g, 2.05 mmol) with stirring (0.5 h), after which a green solid separated from a blue supernatant. Then oxygen was aspirated through the tube and the blue supernatant added with stirring. After 15 min, the cold bath was removed. After 90 min, the mixture was poured into aqueous HCl (2.0 M, 200 mL), which was extracted with diethyl ether (3 × 150 mL). The combined extracts were dried ($MgSO_4$). The solvents were removed by rotary evaporation to give a brownish oil. The residue was dissolved in a minimum of HCl/EtOH (1:100 v/v) and kept at −35°C. Needles formed, which were collected by filtration, washed with cold EtOH, and air-dried to give **TESC$_{16}$TES** as orange needles (0.286 g, 0.068 mmol, 5% assuming a requirement for two equiv of **HC$_8$TES**), mp 36°C (open or sealed capillary), with the melt turning brown at ca. 78°C and then black at 106°C (closed capillary).

NMR (δ/ppm, $CDCl_3$): ^{1}H (500 MHz) 0.98 (t, $^3J_{HH}$ = 7.9 Hz, 18H, C$\underline{H}_3$), 0.64 (q, $^3J_{HH}$ = 7.9 Hz, 12H, SiC$\underline{H}_2$); ^{13}C{^{1}H} (126 MHz, cryoprobe) 88.7 (s, $\underline{C}$≡CSi) [29], 88.3 (s, C≡$\underline{C}$Si) [29], 63.3, 63.1, 63.0, 62.7, 62.5, 61.6 (6 s, SiC≡C($\underline{C}$≡$\underline{C}$)$_3$), 7.4 (s, SiCH$_2\underline{C}$H$_3$), 4.2 (s, $^1J_{CSi}$ = 56.6 Hz [30], Si$\underline{C}$H$_2$).

IR (powder film, cm^{-1}) 2130/2026 (m/m, $\nu_{C\equiv C}$). MS (APCI$^-$) [31]: 422 ([**TESC$_{16}$TES**]$^-$), 100%).

5.3. *TESC$_{24}$TES*

A three-neck flask was fitted with a gas dispersion tube, charged with **PtC$_{10}$TES** (0.203 g, 0.168 mmol) and THF (200 mL), and cooled to −78°C. A Schlenk flask was charged with CuCl (0.240 g, 2.42 mmol), acetone (20 mL), and TMEDA (0.675 mL, 0.523 g, 4.48 mmol) with stirring (0.5 h), after which a green solid separated from a blue supernatant. Then wet *n*-Bu$_4$N$^+$ F$^-$ (1.0 M in THF, 5 wt% water, 0.08 mL, 0.08 mmol) was added to the three-neck flask with stirring. After 5 min (TLC showed no remaining educt), Me_3SiCl (0.10 mL, 0.84 mmol) and a –35°C pentane solution of "crude **HC$_8$TES**" (see SI; from 8.97 mmol of **TESC$_8$TES** and in ca. 30 mL of pentane; ca. 3 mmol of **HC$_8$TES**) were added. Then oxygen was aspirated through the tube and the blue supernatant slowly added with stirring. After 50 min, hexanes (150 mL) were added. The suspension was filtered through a pad of silica gel (5 × 7 cm, packed in 1:1 v/v acetone/hexanes), which was rinsed (1:1 v/v acetone/hexanes) until the filtrate became colorless. The solvents were removed from the filtrate by rotary evaporation at <10°C. The red-brown residue was chromatographed on a silica gel column (4.5 × 30 cm, packed in hexanes), eluted with a 3:0 to 2:1 v/v hexanes/CH_2Cl_2 gradient. The solvents were removed from the product-containing fractions by rotary evaporation at <10°C to give (in order of elution) (1) **TESC$_{24}$TES** that was further treated as described below, (2) **PtC$_{26}$TES** as a brown-orange solid (0.015 g, 0.011 mmol, 7% based upon **PtC$_{10}$TES**), and (3) **PtC$_{18}$TES** as a dark orange solid (0.035 g, 0.027 mmol, 16% based upon **PtC$_{10}$TES**). The **TESC$_{24}$TES** was recrystallized from acidified ethanol (EtOH/HCl, v/v, 100:1) to give a bright orange solid (0.020 g, 0.039 mmol, 4% assuming a requirement for three equiv of **HC$_8$TES**) that gradually turned brown and eventually black in less than an hour if left at room temperature.

NMR (δ/ppm, $CDCl_3$): ^{1}H (500 MHz, cryoprobe): 1.01 (t, $^3J_{HH}$ = 7.9 Hz, 18H, SiCH$_2$C$\underline{H}_3$), 0.65 (q, $^3J_{HH}$ = 7.9 Hz, 12H, SiC$\underline{H}_2$CH$_3$); ^{13}C{^{1}H} (125 MHz, cryoprobe): 88.73 (s, C≡CSi) [29], 88.70 (s, C≡$\underline{C}$Si) [29], 63.9, 63.8, 63.6, 63.5, 63.4, 63.1, 62.9, 62.5, 62.4, 61.5 (10 s, SiC≡C($\underline{C}$≡$\underline{C}$)$_5$), 7.4 (s, SiCH$_2\underline{C}$H$_3$), 4.2 (s, Si$\underline{C}$H$_2$).

IR (powder film, cm^{-1}) 2126/2012 (m/m, $\nu_{C\equiv C}$). MS (APCI$^-$) [31]: 518 ([**TESC$_{24}$TES**]$^-$), 100%).

5.4. *Crystallizations and X-ray diffraction*

A. A CH_2Cl_2 solution of **TESC$_8$TES** was layered with hexanes and kept at −35°C. After 7 d, colorless blocks were collected and data obtained per Table 3. Cell parameters were determined from 45 data frames taken at widths of 1° and refined with 9705 reflections using APEX3 [32]. Data were corrected for Lorentz and polarization factors, and (using SADABS) [33] crystal decay and absorption effects. The non-centrosymmetric space group (*Pca2$_1$*) was determined from systematic reflection conditions and statistical tests, and was confirmed by SHELXT [34]. Hydrogen atoms were placed in idealized positions and refined using a riding model. All non-hydrogen atoms were refined anisotropically. The Flack parameter was refined to 0.156(9) [35]. The absolute structure was determined using Bayesian statistics on Bijvoet differences, which using Olex2 results in 0.171(9) [36]. The structure was refined (weighted least squares refinement on F^2) to convergence [34,37].

Table 4
Crystallographic distances [Å] and angles [°] for **TESC$_8$TES** and **TESC$_{16}$TES**.

	TESC$_{16}$TES (molecule 1)	**TESC$_{16}$TES** (molecule 2)[a]	**TESC$_8$TES**
Si1-C1	1.855(2)	1.859(2)	1.856(3)
C1≡C2	1.208(3)	1.202(3)	1.210(4)
C2-C3	1.370(3)	1.372(3)	1.365(4)
C3≡C4	1.211(3)	1.211(3)	1.212(4)
C4-C5	1.355(3)	1.358(3)	1.365(4)
C5≡C6	1.212(3)	1.211(3)	1.205(4)
C6-C7	1.356(3)	1.355(3)	1.375(4)
C7≡C8	1.215(3)	1.216(3)	1.206(4)
C8-C9	1.351(3)	1.355(3)	–
C9≡C10	1.212(3)	1.213(3)	–
C10-C11	1.354(3)	1.355(3)	–
C11≡C12	1.215(3)	1.212(3)	–
C12-C13	1.354(3)	1.358(3)	–
C13≡C14	1.209(3)	1.210(3)	–
C14-C15	1.372(3)	1.369(3)	–
C15≡C16	1.206(3)	1.207(3)	–
Cω[b] -Si2	1.853(2)	1.859(2)	1.856(3)
avg. C≡C	1.211	1.210	1.208
avg. C-C	1.359	1.360	1.368
BLA(avg)[c]	0.148	0.150	0.160
BLA[d]	0.138	0.141	0.157
sum, bond lengths, Si1 to Si2	22.908(3)	22.922(3)	12.650(4)
Si1···Si2	22.561	22.484	12.603
Si1-C1-C2	175.9(2)	172.7(2)	174.3(3)
C1-C2-C3	178.9(2)	176.6(2)	178.0(3)
C2-C3-C4	179.3(3)	177.1(2)	177.8(3)
C3-C4-C5	178.9(2)	175.7(2)	178.9(3)
C4-C5-C6	178.6(2)	176.5(2)	178.3(3)
C5-C6-C7	178.9(3)	178.2(2)	178.6(3)
C6-C7-C8	178.1(3)	179.4(2)	179.1(3)
C8-C9-C10	176.2(3)	179.2(2)	–
C9-C10-C11	176.4(3)	179.5(2)	–
C10-C11-C12	176.6(3)	178.5(2)	–
C11-C12-C13	176.7(3)	178.9(2)	–
C12-C13-C14	175.9(2)	177.4(2)	–
C13-C14-C15	177.2(2)	175.7(2)	–
C14-C15-C16	178.2(3)	175.9(3)	–
C(ω–1)-Cω[b] -Si2	175.7(2)	172.7(2)	174.3(3)
avg. bond angle, Si1 to Si2	177.4	177.3	177.3

[a] For this molecule, the atoms are numbered differently from the cif file.
[b] The sp carbon atom connected to the triethylsilyl group.
[c] BLA(avg) = (avg. C-C) − (avg. C≡C).
[d] BLA = absolute value of the length of the central carbon-carbon bond (C≡C for n = odd; C-C for n = even; n = number of C≡C units) minus the average length of the two adjacent bonds.

B. A CH_2Cl_2 solution of **TESC$_{12}$TES** was layered with MeOH and kept at −35°C. After 6 d, microcrystalline dark yellow needles were collected. However, crystals suitable for X-ray analyses could not be obtained.
C. A CH_2Cl_2 solution of **TESC$_{16}$TES** was layered with hexanes and kept at −35°C. After 12 d, orange needles were collected, and data obtained per Table 3. Cell parameters were determined from 45 data frames taken at widths of 1° and refined with 9580 reflections using APEX3 [32]. Data were corrected for Lorentz and polarization factors, and (using SADABS) [33] crystal decay and absorption effects. The space group was determined from systematic reflection conditions and statistical tests, and was confirmed by SHELXT [34]. Elongated thermal ellipsoids on atoms C23-C28 suggested disorder, but modeling efforts did not improve either the reliability factors or thermal ellipsoids. Hydrogen atom positions were placed in idealized positions and refined using a riding model. All non-hydrogen atoms were refined anisotropically. Two independent molecules were found in the unit cell. The structure was refined (weighted least squares refinement on F^2) to convergence [34,37].
D. A CH_2Cl_2 solution of **TESC$_{24}$TES** was layered with hexanes and kept at −35°C. After 14 d, brown microcrystalline needles were collected, which were ground to fine particles of uniform size. The powder was loaded into a two-circle goniometer in a radiation safety enclosure. The X-ray source (1kW Cu tube; 1.54060 Å) was maintained at an operating current of 40 kV and 25 mA. A standard Bragg-Brentano para-focusing mode was used for the optics, with the X-ray diverginssg from a DS slit (1 mm) at the tube to strike the sample and then converging at a position sensitive X-ray Detector (Lynx-Eye, Bruker-AXS). The two-circle 218 mm diameter θ-θ goniometer was computer controlled with independent stepper motors and optical encoders for the θ circle with the smallest angular step size of 0.0001° (2θ). Data collection (see Figure S1) used the automated COMMANDER program and a DQL file. Data were analyzed by the program EVA.

Supplementary data

CCDC 2366801 (**TESC$_8$TES**) and 2366802 (**TESC$_{16}$TES**) contain the supplementary crystallographic data for this paper. These data can be obtained free of charge via www.ccdc.cam.ac.uk/ data_request/cif, or by emailing data_request@ccdc.cam.ac.uk, or by contacting The Cambridge Crystallographic Data Centre, 12 Union Road, Cambridge CB2 1EZ, UK; fax: +44 1223 336033.

Supplementary materials

The synthesis and isolation of **TESC$_8$TES**, generation of pentane solutions of **HC$_8$TES**, and powder XRD, NMR, and mass spectrometric data.

CRediT authorship contribution statement

Sourajit Dey Baksi: Writing – review & editing, Writing – original draft, Visualization, Validation, Methodology, Investigation, Formal analysis, Data curation. **Aayushi Arora:** Writing – review & editing, Writing – original draft, Visualization, Validation, Software, Methodology, Investigation, Formal analysis, Data curation. **Nattamai Bhuvanesh:** Validation, Software, Resources, Methodology. **Joseph H. Reibenspies:** Validation, Software, Resources, Methodology. **John A. Gladysz:** Writing – review & editing, Writing – original draft, Visualization, Validation, Supervision, Resources, Project administration, Funding acquisition, Conceptualization.

Declaration of competing interest

The authors declare no competing financial interest.

Data availability

Data will be made available on request.

Acknowledgements

The US National Science Foundation (NSF; CHE-1900549) and Welch Foundation (A-2189) are thanked for support.

Supplementary materials

Supplementary material associated with this article can be found, in the online version, at doi:10.1016/j.jorganchem.2024.123308.

References

[1] a) For synthetic milestones, see W.A. Chalifoux, R.R. Tykwinski, Synthesis of extended polyynes: toward carbyne, Comptes Rendus Chimie 12 (2009) 341–358, https://doi.org/10.1016/j.crci.2008.10.004;
b) Y. Gao, R.R. Tykwinski, Advances in polyynes to model carbyne, Acc. Chem. Res. 55 (2022) 3616–3630, https://doi.org/10.1021/acs.accounts.2c00662.
[2] a) C.-F. Lv, X.-G. Yang, C.-X. Shan, One-dimensional sp carbon: synthesis, properties, and modifications, Chin. Phys. B 31 (2022) 128103, https://doi.org/10.1088/1674-1056/ac872f;
b) B. Pan, J. Xiao, J. Li, P. Liu, C. Wang, G. Yang, Carbyne with finite length: the

one-dimensional *sp* carbon, Sci. Adv. 1 (2015) e1500857, https://doi.org/10.1126/sciadv.1500857.

[3] a) W.A. Chalifoux, R.R. Tykwinski, Synthesis of polyynes to model the *sp*-carbon allotrope carbyne, Nature Chem 2 (2010) 967–971, https://doi.org/10.1038/nchem.828;
b) Y. Gao, Y. Hou, F.G. Gárnez, M.J. Ferguson, J. Casado, R.R. Tykwinski, The loss of endgroup effects in long pyridyl-endcapped oligoynes on the way to carbyne, Nature Chem 12 (2020) 1143–1149, https://doi.org/10.1038/s41557-020-0550-0.

[4] A. Arora, S. Dey Baksi, N. Weisbach, H. Amini, N. Bhuvanesh, J.A. Gladysz, Monodisperse molecular models for the sp carbon allotrope carbyne; syntheses, structures, and properties of diplatinum polyynediyl complexes with $PtC_{20}Pt$ to $PtC_{52}Pt$ linkages, ACS Cent. Sci. 9 (2023) 2225–2240, https://doi.org/10.1021/acscentsci.3c01090.

[5] C.W. Patrick, Y. Gao, P. Gupta, A.L. Thompson, A.W. Parker, H.L. Anderson, Masked alkynes for synthesis of threaded carbon chains, Nature Chem 16 (2024) 193–200, https://doi.org/10.1038/s41557-023-01374-z.

[6] M.R. Bryce, A review of functional linear carbon chains (oligoynes, polyynes, cumulenes) and their applications as molecular wires in molecular electronics and optoelectronics, J. Mater. Chem. C 9 (2021) 10524–10546, https://doi.org/10.1039/D1TC01406D.

[7] a) R.-S. Zhang, J.-W. Jiang, The art of designing carbon allotropes, Front. Phys. 14 (2019) 13401, https://doi.org/10.1007/s11467-018-0836-5;
b) Q. Fan, H. Liu, C. Ren, S. Yun, U. Schwingenschlögl, High-throughput design of three-dimensional carbon allotropes with P*mna* space group, Materials Today Advances 22 (2024) 100486, https://doi.org/10.1016/j.mtadv.2024.100486.

[8] R. Eastmond, T.R. Johnson, D.R.M. Walton, Silylation as a protective method for terminal alkynes in oxidative couplings, Tetrahedron 28 (1972) 4601–4616, https://doi.org/10.1016/0040-4020(72)80041-3.

[9] T.R. Johnson, D.R.M. Walton, Silylation as a Protective Method in Acetylene Chemistry, Tetrahedron 28 (1972) 5221–5236, https://doi.org/10.1016/S0040-4020(01)88941-9.

[10] a) F. Bohlmann, Die Polyine, Angew. Chem. 65 (1953) 385–408, https://doi.org/10.1002/ange.19530651502;
b) E.R.H. Jones, H.H. Lee, M.C. Whiting, Researches on acetylenic compounds. Part LXIV. The preparation of conjugated octa- and deca-acetylenic compounds, J. Chem. Soc. (1960) 3483–3489, https://doi.org/10.1039/JR9600003483;
c) A.M. Sladkov, Y.P. Kudryavtsev, Polyynes, Russ. Chem. Rev. 32 (1963) 229–243, https://doi.org/10.1070/RC1963v032n05ABEH001338.

[11] A.S. Hay, Oxidative couplings of acetylenes. II, J. Org. Chem. 27 (1962) 3320–3321, https://doi.org/10.1021/jo01056a511.

[12] S. Eisler, A.D. Slepkov, E. Elliott, T. Luu, R. McDonald, F.A. Hegmann, R. R. Tykwinski, Polyynes as a model for carbyne: synthesis, physical properties, and nonlinear optical response, J. Am. Chem. Soc. 127 (2005) 2666–2676, https://doi.org/10.1021/ja044526l.

[13] D.R. Kohn, P. Gawel, Y. Xiong, K.E. Christensen, H.L. Anderson, Synthesis of polyynes using dicobalt masking groups, J. Org. Chem. 83 (2018) 2077–2086, https://doi.org/10.1021/acs.joc.7b03015.

[14] Y. Rubin, S.S. Lin, C.B. Knobler, J. Anthony, A.M. Boldi, F. Diederich, Solution-spray flash vacuum pyrolysis: a new method for the synthesis of linear poliynes with odd numbers of C≡C bonds from substituted 3,4-dialkynyl-3-cyclobutene-1,2-diones, J. Am. Chem. Soc. 113 (1991) 6943–6949, https://doi.org/10.1021/ja00018a035.

[15] a) R.C. DeCicco, A. Black, L. Li, N.S. Goroff, An iterative method for the synthesis of symmetric polyynes, Eur. J. Org. Chem. (2012) 4699–4704, https://doi.org/10.1002/ejoc.201200442;
b) D.C. Milan, O.A. Al-Owaedi, M.-C. Oerthel, S. Marqués-González, R.J. Brooke, M.R. Bryce, P. Cea, J. Ferrer, S.J. Higgins, C.J. Lambert, P.J. Low, D.Z. Manrique, S. Martin, R.J. Nichols, W. Schwarzacher, V.M. García-Suárez, Solvent dependence of the single molecule conductance of oligoyne-based molecular wires, J. Phys. Chem. C 120 (2016) 15666–15674, https://doi.org/10.1021/acs.jpcc.5b08877.

[16] Y. Tobe, R. Umeda, N. Iwasa, M. Sonoda, Expanded Radialenes with Bicyclo[4.3.1] decatriene Units: New Precursors to Cyclo[n]carbons, Chem. Eur. J. 9 (2003) 5549–5559, https://doi.org/10.1002/chem.200305051.

[17] For efforts in this direction, see W.A. Chalifoux, M.J. Ferguson, R.R. Tykwinski, Tris(biphenyl-4-yl)silyl-Endcapped Polyynes, Eur. J. Org. Chem. (2007) 1001–1006, https://doi.org/10.1002/ejoc.200600878.

[18] Additional literature: F. Yonehara, Y. Kido, M. Yamaguchi, Unusually high *ortho*-selectivity in electrophilic aromatic substitution promoted by $GaCl_3$ Chem. Commun. (2000) 1189–1190, https://doi.org/10.1039/B003215H.

[19] See footnote s11 of reference [4]. The **$TESC_8TES$** elutes first from silica gel, but quantitative separations from **HC_8TES** are seldom achieved. The **HC_8H** elutes last while partially decomposing (sometimes with a noticeable exotherm) on the column.

[20] B. K. Collins, J. A. Gladysz, submitted to *Chem. Eur. J.*

[21] Synthesis of a mixture containing $TESC_6TES$: I. Curbet, S. Colombel-Rouen, R. Manguin, A. Clermont, A. Quelhas, D.S. Müller, T. Roisnel, O. Baslé, Y. Trolez, M. Mauduit, Expedient synthesis of conjugated triynes *via* alkyne metathesis Chem. Sci. 11 (2020) 4934–4938, https://doi.org/10.1039/D0SC01124J.

[22] R. Dembinski, T. Bartik, B. Bartik, M. Jaeger, J.A. Gladysz, Toward Metal-Capped One-Dimensional Carbon Allotropes: Wirelike C_6-C_{20} Polyynediyl Chains That Span Two Redox-Active (η^5-C_5Me_5)Re(NO)(PPh_3) Endgroups, J. Am. Chem. Soc. 122 (2000) 810–822, https://doi.org/10.1021/ja992747z.b)Please see the general cautionary note regarding polyynes in the experimental section. We have yet to experience any problems with **BrC_4Br**, although it is a strong lachrymator.

[23] S. Radhika, N.A. Harry, M. Neetha, G. Anilkumar, Recent trends and applications of the Cadiot-Chodkiewicz reaction, Org. Biomol. Chem. 17 (2019) 9081–9094, https://doi.org/10.1039/C9OB01757G.

[24] a) M. Nobis, J. Futter, M. Moxter, S. Inoue, B. Rieger, Photo-activity of silacyclopropenes and their application in metal-free curing of silicones, ChemSusChem 16 (2022) e202201957, https://doi.org/10.1002/cssc.202201957;
b) J. Szyling, A. Szymańska, A. Franczyk, J. Walkowiak, [$Pt(PPh_3)_4$]-catalyzed selective diboration of symmetrical and unsymmetrical 1,3-Diynes, J. Org. Chem. 87 (2022) 10651–10663, https://doi.org/10.1021/acs.joc.2c00844 (see the supporting information therein).

[25] F. Zhuravlev, J.A. Gladysz, Electronic structure and chain-length effects in diplatinum polyynediyl complexes *trans,trans*-[$(X)(R_3P)_2Pt(C{\equiv}C)_nPt(PR_3)_2(X)$]: a computational investigation, Chem. Eur. J. 10 (2004) 6510–6522, https://doi.org/10.1002/chem.20040064.

[26] See also Figure 5 of Q. Zheng, J.C. Bohling, T.B. Peters, A.C. Frisch, F. Hampel, J. A. Gladysz, A synthetic breakthrough into an unanticipated stability regime: a series of isolable complexes in which C_6, C_8, C_{10}, C_{12}, C_{16}, C_{20}, C_{24}, and C_{28} Polyynediyl chains span two platinum atoms, Chem. Eur. J. 12 (2006) 6486–6505, https://doi.org/10.1002/chem.200600615.

[27] H. Amini, N. Weisbach, S. Gauthier, H. Kuhn, N. Bhuvanesh, F. Hampel, J. H. Reibenspies, J.A. Gladysz, Trapping of terminal platinapolyynes by Copper(I) catalyzed click cycloadditions; probes of labile intermediates in syntheses of complexes with extended sp carbon chains, and crystallographic studies, Chem. Eur. J. 27 (2021) 12619–12634, https://doi.org/10.1002/chem.202101725.

[28] a) G.E. Jones, D.A. Kendrick, A.B. Holmes, 1,4-BIS(TRIMETHYLSILYL)BUTA-1,3-DIYNE, Org. Synth. 65 (1987) 52–59, https://doi.org/10.15227/orgsyn.065.0052;
b) W. de Graaf, A. Smits, J. Boersma, G. van Koten, W.P.M. Hoekstra, Synthesis of Marasin and 9-Me-Marasin (Nona- and Deca-6,8-diyne-3,4-dienol), Tetrahedron 44 (1988) 6699–6704, https://doi.org/10.1016/S0040-4020(01)90110-3;
c) S. Bock, P.J. Low, A Safe and Simple Synthesis of 1,4-Bis(trimethylsilyl)buta-1,3-diyne, Aust. J. Chem. 71 (2018) 307–310, https://doi.org/10.1071/CH17402;
d) D.F. Perepichka, S. Jeeva, Chemical safety: trimethylsilylacetylene explosion, Chem. Eng. News 88 (2010) 2. http://cen.acs.org/articles/88/i3/Chemical-Safety-Trimethylsilylacetylene-Explosion.html.

[29] This signal is assigned by analogy to chemical shift trends established for **$TIPSC_8TIPS$** in reference [12].

[30] This coupling represents a satellite (d; $^{29}J_{Si}$ = 4.67%), and is not reflected in the peak multiplicity given.

[31] m/*Z*, most intense peak of the isotope envelope.

[32] *APEX3*, "Program for Data Collection on Area Detectors, BRUKER AXS Inc., Madison, WI, USA, 2012.

[33] G. M. Sheldrick, *SADABS, Program for Absorption Correction for Data from Area Detector Frames*, Bruker AXS Inc., Madison, WI 53711-5373 USA.

[34] a) G.M. Sheldrick, SHELXT – Integrated space-group and crystal structure determination, Acta Cryst A71 (2015) 3–8, https://doi.org/10.1107/S2053273314026370;
b) G.M. Sheldrick, Crystal structure refinement with *SHELXL*, Acta Cryst. C71 (2015) 3–8, https://doi.org/10.1107/S2053229614024218.

[35] H.D. Flack, On enantiomorph-polarity estimation, Acta Cryst A39 (1983) 876–881, https://doi.org/10.1107/S0108767383001762 (theory for correct and inverted configurations: 0 and 1).

[36] a) R.W.W. Hooft, L.H. Straver, A.L. Spek, Determination of absolute structure using Bayesian statistics on Bijvoet differences, J. Appl. Cryst. 41 (2008) 96–103, https://doi.org/10.1107/S0021889807059870;
b) A.L. Thompson, D.J. Watkin, X-ray crystallography and chirality: understanding the limitations, Tetrahedron: Asymmetry 20 (2009) 712–717, https://doi.org/10.1016/j.tetasy.2009.02.025.

[37] O.V. Dolomanov, L.J. Bourhis, R.J. Gildea, J.A.K. Howard, H. Puschmann, OLEX2: a complete structure solution, refinement and analysis program, J. Appl. Cryst. 42 (2009) 339–341, https://doi.org/10.1107/S0021889808042726.